Article

The natural product rotundic acid treats both aging and obesity by inhibiting PTP1B

Jie Zhu[1,2,‡], Yongpan An[1,‡], Xin Wang[1,‡], Liting Huang[2], Weikaixin Kong[3], Miaomiao Gao[1], Jingxiang Wang[1], Xinpei Sun[1], Sujie Zhu[2,*], Zhengwei Xie[1,4,*]

[1]Peking University International Cancer Institute and Department of Pharmacology, School of Basic Medical Sciences, Peking University, Beijing 100191, China
[2]Institute of Translational Medicine, The Affiliated Hospital of Qingdao University, College of Medicine, Qingdao University, Qingdao 266021, China
[3]Institute for Molecular Medicine Finland (FIMM), University of Helsinki, Helsinki 00014, Finland
[4]Peking University - Yunnan Baiyao International Medical Research Center, Peking University Health Science Center, Beijing 100191, China
[‡]These authors contributed equally to this work.
[*]Correspondence: zhusujie@qdu.edu.cn (S.Z.), xiezhengwei@hsc.pku.edu.cn (Z.X.)
Received: 3 July 2022; Accepted: 20 October 2022.
https://doi.org/10.1093/lifemedi/lnac044

Keywords: aging; obesity; rotundic acid; PTP1B; leptin

The occurrence of obesity is associated with age. But their interplay remains mysterious. Here, we discovered that rotundic acid (RA), a plant-derived pentacyclic triterpene, was a powerful agent for both anti-aging and treating obesity. Considering that obese individuals decrease the appetite-suppressing and energy-expenditure-enhancing functions of leptin leading to obesity, we found RA was a leptin sensitizer, evidenced by observations that RA enhanced the leptin sensitivity to normal diet-induced obese (DIO) mice, and had minimal or no use to normal lean mice, leptin receptor-deficient (db/db) mice, and leptin-deficient (ob/ob) mice. Simultaneously, RA significantly increased energy expenditure, BAT thermogenesis, and glucose metabolism in DIO mice, as the results of enhancing leptin sensitivity. Regarding mode of action, we demonstrated that RA is a noncompetitive inhibitor of leptin negative regulators protein tyrosine phosphatase 1B (PTP1B) and T-cell PTP through interaction with their C-terminus, thus leading to weight loss through enhancing leptin sensitivity. Besides, we showed that deletion of yPTP1 in yeast completely abolished the lifespan extension effect of RA, celstrol, and withaferin A, while these compounds exhibited PTP1B inhibition activity. Furthermore, PTP1B knockdown extend lifespan in yeast and human cells, indicating PTP1B is an important factor regulating cellular aging.

Introduction

The probability of being obese is positively correlated with human age [1]. Obesity and aging share a similar spectrum of phenotypes including impaired mitochondrial function, weakened immunity, shifts in tissue and body composition, and enhanced systemic inflammation. Adults with obesity are at higher risk of a number of age-related conditions and diseases including cardiovascular disease (CVD), hypertension, type 2 diabetes mellitus, and cancer [2, 3]. Increasing abdominal obesity, often observed in the process of aging, is understood as a major contributor to insulin resistance and metabolic syndrome. Moreover, it has been shown that obesity increases the risk of premature death by 1.45 to 2.76-folds, and shortens lifespan by up to 20 years [4, 5]. Thus, obesity apparently accelerates aging at multiple levels.

Leptin is an adipocyte-derived hormone critical for both energy homeostasis and body weight control [6, 7]; leptin acts on neurons in brain areas such as the hypothalamus, hippocampus, and brain stem, and regulates food intake, thermogenesis, energy expenditure (EE), and homeostasis of glucose/lipid metabolism. Aberrantly increased circulating leptin levels are common in obese individuals, and such increases are used as a biomarker of leptin resistance. Leptin resistance—defined as a reduced sensitivity or a failure of the brain to respond to leptin—decreases the appetite-suppressing and energy-expenditure-enhancing functions of leptin, resulting in increased food intake and finally causing obesity, CVDs, and other metabolic disorders. Notably, the hyperleptinemic state of obesity can be leveraged for therapeutic purposes by increasing leptin sensitivity [8, 9]. There are reports of leptin resistance is also observed in aged individuals [10, 11]. Older

individuals have higher leptin mRNA levels than young ones. Studies on resistance to leptin administration revealed that old rats (30 months of age) with elevated adiposity presented 3-fold greater endogenous serum leptin levels than young individuals (6 months of age) [12, 13]. Youth is associated with sensitivity to leptin, while aging is linked with a failure in leptin action, independently of obesity or body fat distribution [13, 14]. Such clues imply that perturbation of leptin may modulate aging, although this supposition has not been experimentally demonstrated with a modulatory agent [15].

PTPs such as PTP1B or T-cell PTP (TCPTP) participated in leptin receptor signaling. PTP1B is a tyrosine phosphatase that dephosphorylates Janus-activated kinase (JAK)-2 to suppress the activating tyrosine phosphorylation of the growth-related transcription factor STAT3 [16]; while hypothalamic PTP1B knockdown or administration of PTP1B inhibitors enhance leptin sensitivity, decrease weight gain, and improve insulin sensitivity in rodent models of obesity [17, 18]. At the same time, studies have shown that PTP1B was downregulated by SIRT1 which played important role in improving health during aging [19]. Resveratrol improves insulin sensitivity by repressing PTP1B and extends the lifespan of diet-induced obese (DIO) mice [20, 21]. These findings promote the view that PTP1B may be a promising target for treating obesity, diabetes, and aging. TCPTP, is closely related to PTP1B, sharing a high degree of primary (72% identity) and tertiary structural similarity [22]. Hypothalamic TCPTP levels are increased in obesity acting together with elevated PTP1B in the attenuation of leptin signal and the development of cellular leptin resistance. Inhibition of TCPTP in C57BL/6 mice enhanced leptin-induced hypothalamic STAT3 signaling and increased the effects of leptin on body weight and EE [23].

Some natural compounds exert both anti-obesity and anti-aging effects, such as berberine increases EE, limits weight gain, enhances brown adipose tissue (BAT) activity, and extends lifespan [24, 25]; urolithin A exerts anti-obesity in mice and prolongs lifespan in *C. elegans* [26, 27]. More and more natural compounds have shown dual activity in resisting obesity and prolonging the lifespan. Rotundic acid (RA), a pentacyclic triterpenoid compound, exerts anti-inflammatory, cardio-protective, and anti-tumor effects [28, 29]. Here, we report that RA is a powerful agent to treat both aging and obesity. We demonstrate that RA confers 135% lifespan extension in yeast and 16.2% extension in mice. In the DIO model, we found that RA treatment of these hyperleptinemic mice suppressed food intake while increasing both BAT thermogenesis and white adipose tissue (WAT) browning, EE and improving glucose metabolism, finally leading to 26% weight loss in the DIO model mice. Mechanistically, we discovered that these effects result from RA's noncompetitive inhibition of PTP1B and TCPTP activity, which increased leptin and insulin sensitivity. As expected, RA had no weight-reducing effect on leptin receptor-deficient (db/db) mice, leptin-deficient (ob/ob) mice, or normal lean mice. Notably, considering the anti-aging effect of RA, we confirmed that PTP1B knockdown extends the lifespan. Taken together, our study demonstrates how RA functions as a leptin sensitizer and illustrates its promising applications as a promising agent for treating aging and obesity.

Results

RA significantly extends the lifespan of yeast and mice

The genesis of this study was the use of our newly developed deep learning-based efficacy prediction system (DLEPS) [30] to computationally screen for potential anti-aging compounds. DLEPS used the disease-specific gene signatures to calculate an enrichment score similar to that in connectivity map [9]. Herein, since muscle is an important indicator of aging and also plays a critical role on sugar and fat metabolism, we finally used up/down aging gene signatures analyzed from aged and young human muscles [31] (Fig. S1A) to explore the lifespan extending's effect of drugs. We then picked three top-ranked small molecules (Fig. 1A) for experimental validation.

We first employed a microfluidic chip-based device, mounted on a time-lapse microscope, to measure the replicative lifespan of yeast [32]. Specifically, cells were taken from solid YEPD media and incubated in the SD media for 20 h, harvested, and loaded onto the chip, where the cells were continuously incubated with SD medium with or without drugs, and were monitored continuously with microscopic imaging for 48 h. We tested three small molecules, among which the pentacyclic triterpene RA (Fig. S1B) was able to significantly extend the yeast lifespan. Subsequent assessment of lifespan in the presence of 3.125, 6.25, 12.5, 25, 50, or 100 μM RA showed that all of the tested concentrations significantly extended the lifespan of yeast to a similar extent (14.8–19.35 generations and 103%–135%, Fig. 1B), although the maximum detected increase was for the 12.5 μM dose (corresponding to the extension of 19.35 generations and 135%; Fig. 1B). We also noted that the proportion of cells displaying long cell-cycle duration was significantly reduced by RA treatment (green-colored cells in Fig. 1C). Based on these results, we then checked the anti-aging effects in the WI-38 human embryonic lung fibroblast cell line, since it has been a cell line commonly using in the study of aging. Notably, 12.5 μM RA showed stronger effects on proliferation of senescent WI-38 cells (PD40; Fig. S1C). We further performed SA-β-gal staining to assess cellular senescence, revealing that RA significantly reduced SA-β-gal staining after 24 h in WI-38 cells (Fig. 1D).

Next, we tested if RA could extend the lifespan of mice. We started with 16-month-old C57BL/6J male mice and divided them randomly into the control and treatment groups. We observed that RA significantly extends the mean (median) lifespan of mice by 126 (135) days and 16.2% (14.3%), from 776 (946) days to 902 (1081) days (Fig. 1E, left), equivalent to human 11.9 years, using 73.6 years as the mean human lifespan [33]. Residual lifespan analysis showed that RA treatment extended the mean and median lifespan values by 29.0% and 44.2% (See Methods for

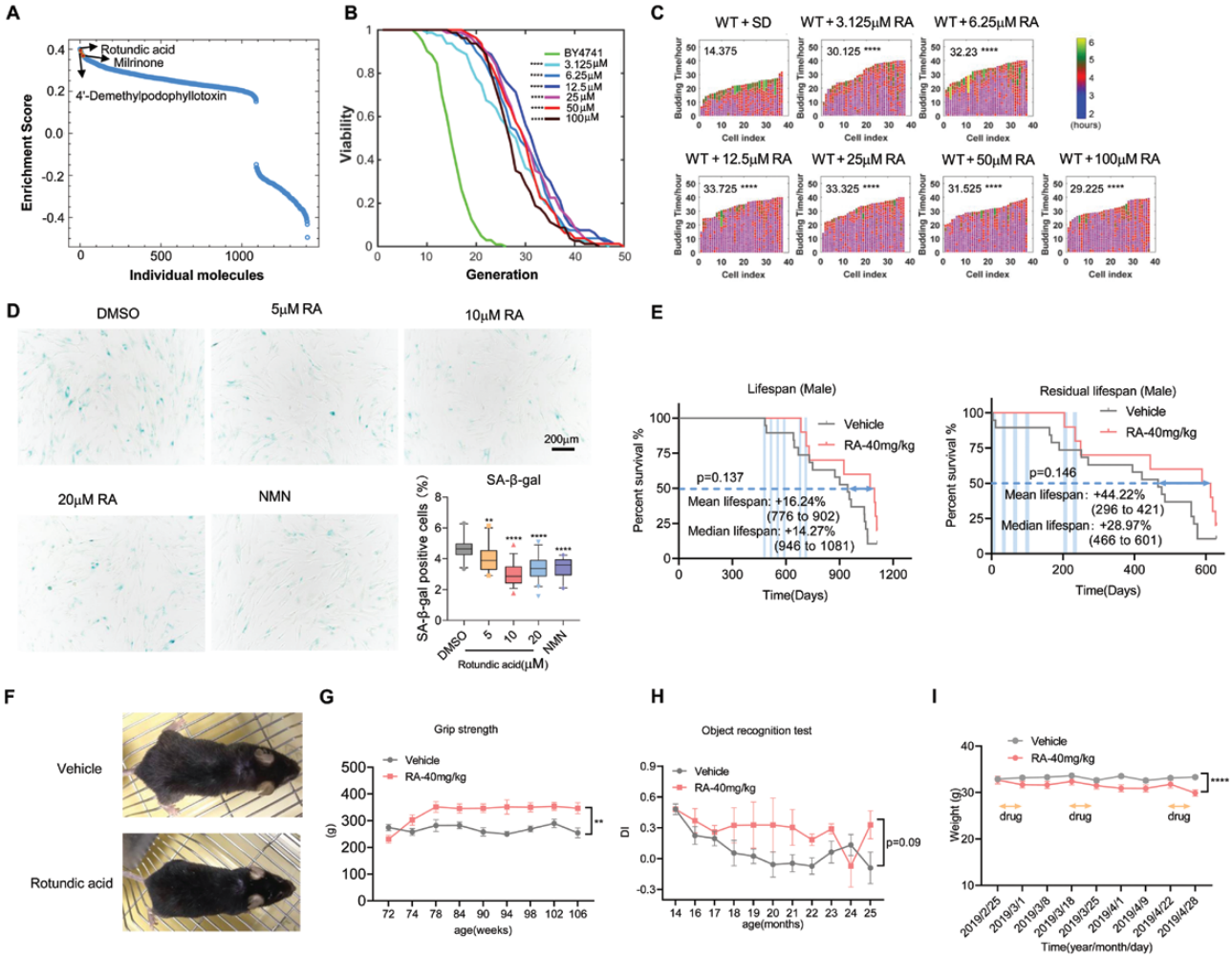

Figure 1. RA significantly extended the lifespan of yeast and naturally aged mice.

(A) Prediction of anti-aging efficacy using a DLEPS. Red dots indicate tested small molecules. (B and C) Effects of RA on the lifespan of yeast. (B) RA-treated mother cells showed an extended replicative lifespan by 14.8–19.35 generations (103%–135% extension) as compared to wild-type cells in SD medium at 3.125, 6.25, 12.5, 25, 50, and 100 μM (The lifespan of 120 yeast cells were counted for each group). (C) Mother cell budding profiles of wild-type and RA-treated cells, showing cell-cycle duration and heterogeneity (see exponential color scale; cell cycles with durations 1.4 h or less were colored in purple; The lifespan of 120 yeast cells were counted for each group). The *x*-axis displays individual mother cells shown as vertical bars. (D) WI-38 cells stained for SA-β-gal following DMSO, 5, 10, 20 μM RA and 1 mM Nicotinamide mononucleotide (NMN; positive control) treatment. The scale bar indicates 200 μm, $n = 3$ per group. *P* values were determined by a one-way ANOVA test. (*$P < 0.05$, **$P < 0.01$, ***$P < 0.001$, ****$P < 0.0001$). (E–I) 16-month-old mice were treated with vehicle ($n = 19$) or RA ($n = 10$) 1 week a month for 6 months. (E) The survival curve of mice treated with RA or vehicle control, starting from birth (left); from the treatment (right), shaded windows showed the administration periods. (F) The representative pictures of 20 months of naturally aged mice treated with 40 mg/kg RA show differential fur density. (G) Grip strength, (H) Discrimination index in the object recognition test. (I) The change in body weight in mice treated with 40 mg/kg RA.

details), respectively (Fig. 1E, right). We also observed that the RA-treated animals had denser fur that had a relatively more lustrous appearance compared to the control mice (Fig. 1F). We further detected that RA treatment led to significantly improved grip strength (Fig. 1G) and significantly delayed decline for discrimination index (DI) values in an object recognition test (Fig. 1H), and we observed no differences between control vehicle-treated and RA-treated aging mice in Y maze test (Fig. S1D). Thus, RA treatment can significantly extend the lifespan of yeast, human cell, showing potential anti-aging effect for mice.

RA ameliorates obesity in DIO mice

During the administration of RA, we surprisingly found that RA-treated mice had a weight-reducing effect (Fig. 1I). We thus planned the following experiments to assess its apparent anti-obesity effects: we treated two groups of DIO model mice, with mean body weights equal to 38 and 58 g, with either vehicle or RA (40 mg/kg; intraperitoneally injection, daily for 2 weeks). RA treatment significantly reduced body weights in both groups (Fig. 2A and 2B, 2D and 2E). At the end of treatment, the body weight of the RA-treated DIO mice in these two groups were respectively

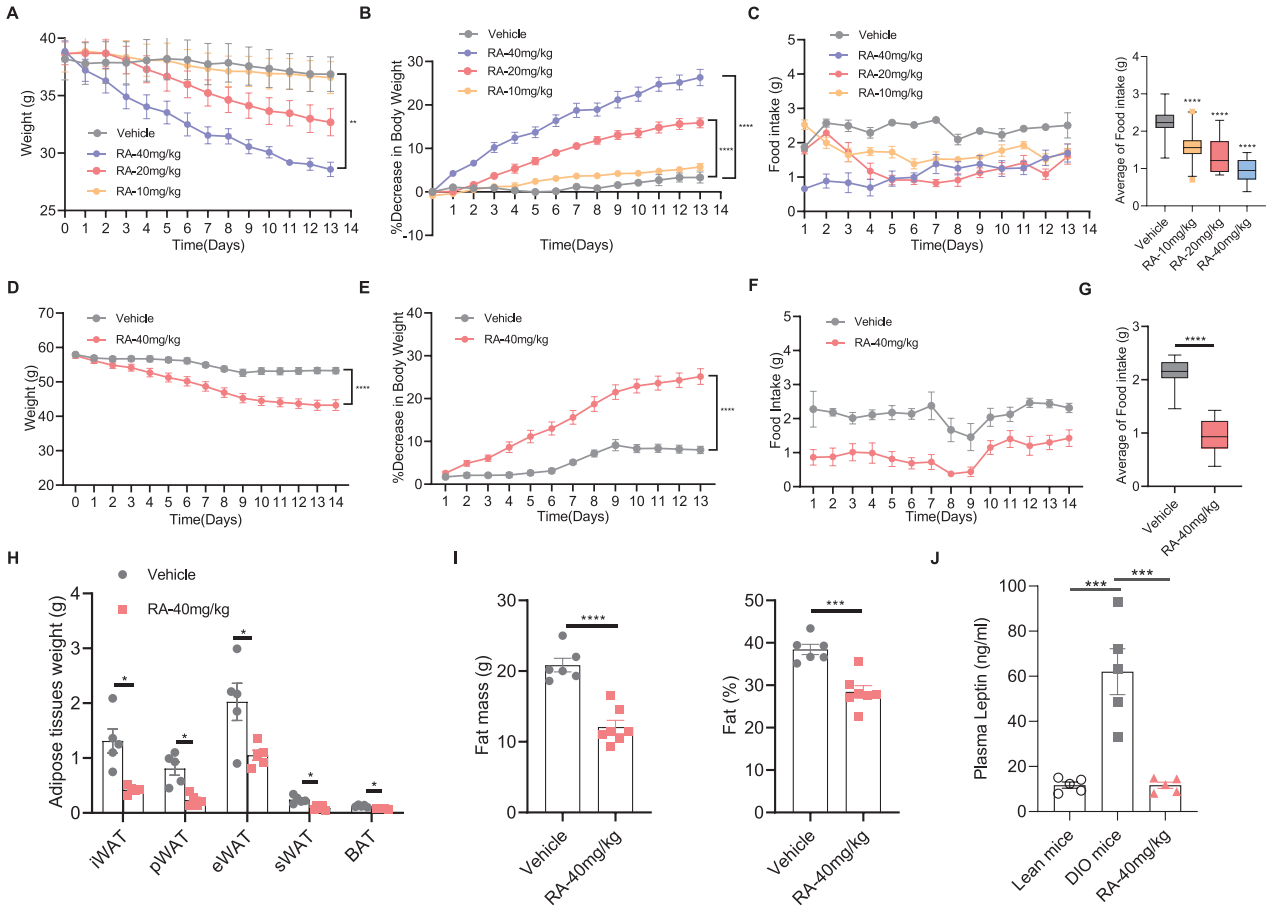

Figure 2. RA acts as an anti-obesity agent on high fat diet-induced obese mice.

DIO mice (body weight ~38 g) were treated daily with vehicle or RA (10/20/40 mg/kg) via intraperitoneal (i.p.) injection for 2 weeks. (A) Body weight (g) and (B) Percent decrease (%) in body weight during treatment (n = 5–7 for each group). (C) Daily food intake (in grams) of DIO mice during the 2 weeks of treatment (left). Average food intake of DIO mice (right) (n = 5–7 for each group). (D–F) DIO mice (body weight ~58 g) were treated daily with vehicle or RA (40 mg/kg) via i.p. injection for 2 weeks. (D) Body weight (g) and (E) percent decrease (%) in body weight in DIO mice during the treatment (n = 7–8 for each group). (F) Daily food intake (g) of DIO mice during 2 weeks of treatment (n = 7–8, left). (G) Average food intake of DIO mice (right). (H) The weights of iWAT, pWAT, eWAT, sWAT, and BAT fat pads were reduced after RA treatment. (I) Fat mass and fat percentage (n = 6–7) decreased after RA treatment. (J) Plasma leptin levels in RA or vehicle-treated DIO model mice and normal lean mice (n = 5 for each group). Data represent the mean ± SEM. P values were determined by one-way ANOVA or Student's t-test. (*P < 0.05, **P < 0.01, ***P < 0.001, ****P < 0.0001).

reduced by 26.3% and 25.1%, whereas only slight changes were observed with the vehicle-treated control mice (Fig. 2B and 2E). Of particular note, the RA treatment (40 mg/kg) caused 62.3% and 60.9% reductions in daily food intake in the two groups during the first week of treatment (Fig. 2C and 2F).

Upon sacrificing the mice of the 58 g group, we observed that RA treatment had significantly reduced the weights of inguinal (iWAT), perinephric (pWAT), epididymal (eWAT), scapular (sWAT), and BAT (Fig. 2H). By applying a magnetic resonance imaging technique, we measured the fat mass and lean mass of the RA-treated and vehicle-treated groups: the fat mass and fat percentage of the mice given RA were significantly (9 g and 35.2%) lower than that of vehicle-treated group (Fig. 2I), while the lean mass did not change (Fig. S2A). Given that leptin is generated by adipocytes [34], and considering our observation that WAT masses were reduced in RA-treated DIO mice, we anticipated that leptin would also be reduced upon RA treatment. Indeed, we observed that leptin was reduced down to close-to-lean levels by the end of the 2-week treatment period in DIO mice (Fig. 2J). These results show that, beyond its anti-aging function, RA is also an effective agent for body weight reduction.

RA minimally affects normal, db/db, and ob/ob mice

Obesity is associated with compromised leptin sensitivity [35], so we hypothesized that RA may exert its function(s) by enhancing leptin sensitivity, perhaps acting as a "leptin sensitizer" [8, 9]. The normal lean mice (~22 g; with low leptin levels), db/db mice (lacking functional leptin receptors), and ob/ob mice (leptin deficiency) represent three distinct experimental models to assess leptin sensitivity. First, we treated the lean mice with vehicle or

RA (40 mg/kg) intraperitoneally for 2 weeks. We observed that RA administration had no effect on the body weight of lean mice when given at doses that were effective in reducing the weight of DIO mice (Fig. 3A). On the contrary, RA-treated lean mice continued to gain weight (Figs. 3A, S3A and S3D). Further, RA treatment did not reduce food intake in lean mice (Figs. 3B and S3E), and we detected no changes in the weights of inguinal, perinephric, epididymal, scapular, and brown fat pads (Figs. 3C, S3B and S3C). There was no significant difference in absolute body weight between the two groups at the end of treatment (Fig. S3G). These findings lend additional support to the possibility that RA may act somehow modulate leptin signaling.

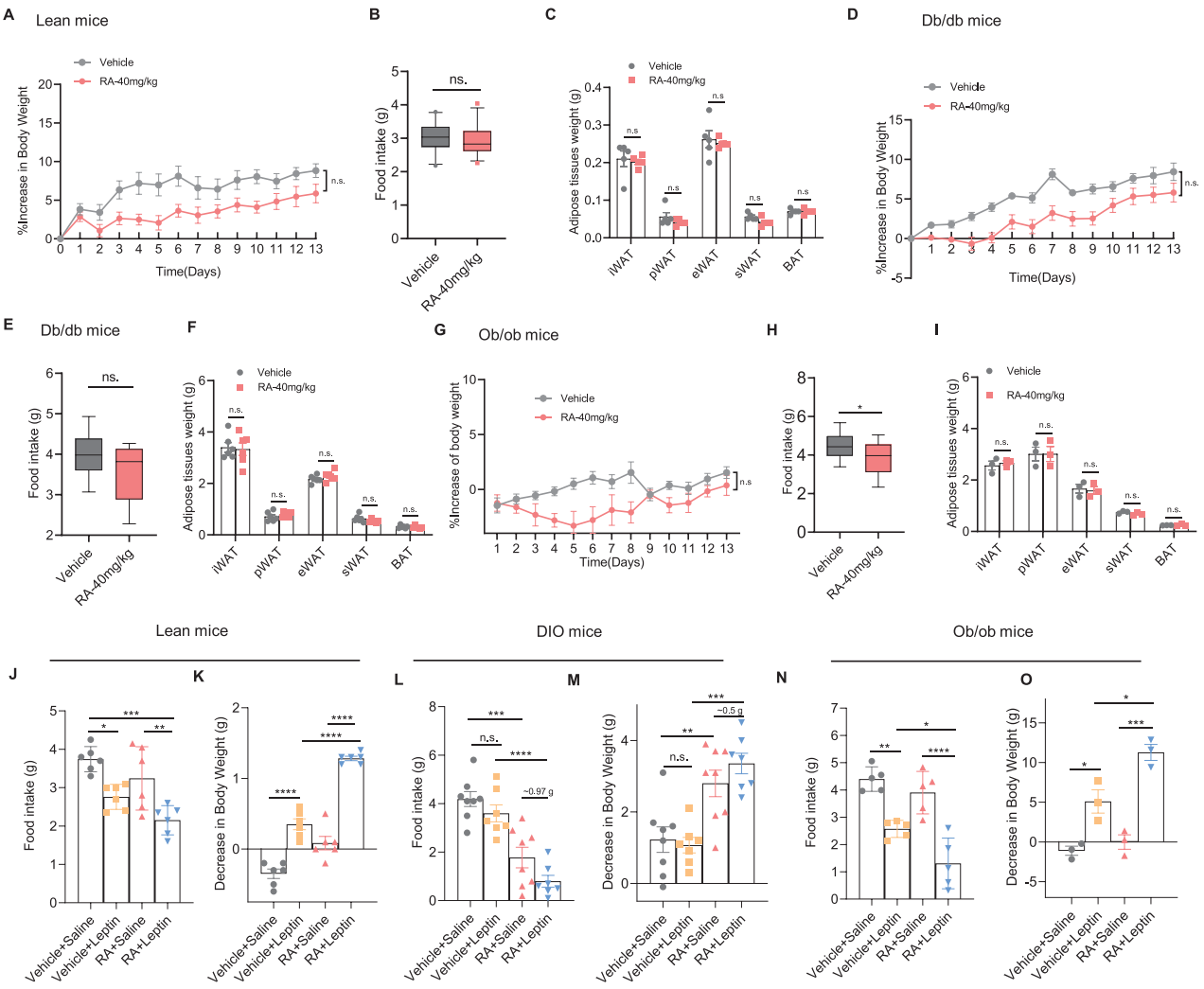

Figure 3. RA acts as a leptin sensitizer.

(A–I) Eight-week-old male normal lean mice (A–C), db/db mice (D–F), and ob/ob mice (G–I) were subjected to a 2-week treatment of vehicle or RA (40 mg/kg) (daily, i.p.). (A) Percentage increase in body weight of lean mice during treatment (n = 11 per group). (B) The average food intake of lean mice was not affected during the 2 weeks of treatment (n = 11 for each group). (C) Weights of iWAT, pWAT, eWAT, sWAT, and BAT were not affected by RA treatment (n = 5 for each group). (D) Percentage increase in bodyweight of db/db mice during the treatment (n = 6 for each group). (E) The average daily food intake is similar in RA or vehicle-treated db/db mice during the 2 weeks of treatment. (F) Weights of iWAT, pWAT, eWAT, sWAT, and BAT. (G) Percentage increase in bodyweight of ob/ob mice during the treatment (n = 6 for each group). (H) The average daily food intake of RA or vehicle-treated ob/ob mice. (I) Weights of iWAT, pWAT, eWAT, sWAT, and BAT (n = 3 for each group). (J and K) Vehicle or RA (40 mg/kg) were administered to normal mice for 2 days, and each group subsequently received saline (n = 6 for each subgroup) or leptin (n = 6 for each subgroup; 5 mg/kg). Food intake (J) and body weight (K) was reduced to the greatest extent in the RA + leptin-treated mice. during the 24 h following saline/leptin injections. (L and M) Vehicle or RA was administered to DIO mice for 2 days, and each group of mice received saline (n = 6 for each subgroup) or leptin (n = 6 for each subgroup) (1 mg/kg). Food intake (L) and body weight change (M) during the 24-h saline/leptin injection period. (N and O) Vehicle or RA was administered to ob/ob mice for 7 days, and each group of mice received saline (n = 3 for each subgroup) or leptin (n = 3 for each subgroup; 0.1 mg/kg). Food intake (N) and body weight change (O) during the 24-h saline/leptin injection period. Data are presented as the mean ± SEM. P values were determined by one-way ANOVA or Student's t-test (*P < 0.05, **P < 0.01, ***P < 0.001, ****P < 0.0001).

Second, we treated the db/db mice and ob/ob mice with vehicle or RA (40 mg/kg) intraperitoneally for 2 weeks. Regarding weight, both the vehicle control and RA-treated db/db mice gradually gained weight throughout the course of the experiment (Figs. 3D and S3H). We observed no differences between control vehicle-treated and RA-treated db/db mice in terms of food intake (Fig. 3E), fat mass percentage (Fig. S3I and S3J), the weights of inguinal, perinephric, epididymal, scapular, or brown fat pads (Fig. 3F) or the final body weight (Fig. S3K) after vehicle or RA treatment. The same RA treatment in leptin-deficient ob/ob mice led to a small decrease in body weight at first week, whereas vehicle-treated ob/ob mice displayed a slight gain in body weight, during the treatment period. At the end of trail, an analysis of percentage changes in the body weight of vehicle-treated and RA-treated ob/ob mice resulted in no significant difference (Figs. 3G and S3L). Food intake in RA-treated ob/ob mice were slightly lower than in the vehicle-treated group (Figs. 3H and S3M), but there was no difference in fat mass and final body weight between the two groups at the end of treatment (Figs. 3I and S3N). The total food intake reduction was much smaller than that seen in mice with DIO.

These results emphasize that RA does not cause weight (or food intake) reduction in normal lean mice, leptin receptor-deficient db/db mice, or leptin-deficient ob/ob mice and also support that the observed anti-obesity effects resulting from RA treatment are mediated via leptin signaling.

RA enhanced leptin sensitivity in lean, DIO, and ob/ob mice

To further explore any relationship(s) between RA and leptin signaling, we conducted experiments in which lean mice were injected with saline (control), a bolus dose of leptin with and without RA pretreatment. In line with our understanding of leptin function, the mice given leptin consumed significantly less food than controls (26.3%, Fig. 3J). Notably, mice that received RA plus leptin consumed the least food (42.5%, Fig. 3J). Regarding body weight, leptin or RA alone only to lean mice resulted in a small amount of decrease in the body weight (0.35 and 0.08 g, respectively, Fig. 3K). Notably, administration of leptin to lean mice that were pretreated with RA led to much more body weight loss (1.283 g, Fig. 3K). These results suggest that RA enhanced the sensitivity of leptin in reducing weight in lean mice.

To investigate whether RA also acutely enhances the anorectic and weight-reducing effects of exogenous leptin in DIO mice model, we performed the assessment of the response to leptin in the presence and absence of RA in DIO mice model. Administration of leptin to DIO mice did not significantly alter their food intake, compared to the control group (Fig. 3L), while RA treatment alone reduced the food intake of DIO mice to 42.4%, and administration of leptin to DIO mice that were pretreated with RA led to a further reduction (to 9.1%) in food intake (Fig. 3L). Furthermore, treatment with leptin alone did not significantly change the body weights of DIO mice (Fig. 3M), while RA treatment alone led to a significant (2.80 g) decrease in body weight of DIO mice (Fig. 3M). Note that it is very hard to lower body weight in DIO mice, our results showed DIO mice in the RA plus leptin group lost 3.35 g of body weight, which was lower than all of the other groups (Fig. 3M).

Ob/ob mice are sensitive to the administration of exogenous leptin. We chose a low dose of leptin according to the previous study [8, 9], which is slightly effective (but significantly) in the ob/ob mice, to investigate whether RA can also increase the sensitivity of ob/ob mice to the low doses of leptin. Leptin treatment in the vehicle group led to a 41.5% lower food intake relative to that for the vehicle + saline group. However, the same dose of leptin in the RA-treated group lead to a 66.7% lower food consumption when compared to the RA and saline group (Fig. 3N). Administration of Leptin to ob/ob mice lead to slightly (but significantly) loss of body weight when compared with the vehicle + saline group (Fig. 3O). RA treatment alone did not cause little weight loss. However, the RA + leptin group lost significantly more weight (11.27%) than did the RA + saline (–0.01%) and vehicle + leptin (5.09%) groups. Thus, the body weight and food intake data clearly show that RA enhances the leptin sensitivity of both lean and obese mice.

RA enhanced EE in DIO and normal mice

Beyond its known role in reducing food intake, leptin has also been reported to maintain high-EE [35, 36]. Our observations about RA reduced the fat mass in DIO model mice supported our reasoning that RA, despite its robust effects on reducing food intake, may actually enhance EE. Pursuing this, we measured oxygen consumption (VO_2), EE, and the respiratory quotient in vehicle and RA-treated DIO mice (these experiments included 2 and 7 days treatment windows, and assessed the metabolic phenotypes in calorimetry cages over a 24-h period that included a 12-h day and a 12-h night).

We observed that the VO_2 (Fig. 4A), the carbon dioxide production (VCO_2, Fig. 4B, and EE (Fig. 4C) all significantly increased in the RA-treated group during both light and dark periods. Further, there was a significant decrease in the respiratory exchange ratio (RER; defined as VCO_2/VO_2) in the RA group, again during the light and dark periods (Fig. 4D), a finding indicating that RA-treated mice have apparently adapted their metabolism to utilize fatty acids rather than glucose as their main energy source [8].

Note that we also used the calorimetry cages to examine the aged mice from the ongoing lifespan experiment. Specifically, we examined 24-months old mice (at the end of the 6-months RA treatment window) and found that compared with the vehicle controls, the VO_2, VCO_2, and EE values were all significantly increased in the RA-treated animals, during both the light and dark periods (Fig. S4A–S4E). Again, consistent with the calorimetry findings for the DIO model mice, we found that the RER was significantly decreased in the RA-treated normal aged mice (Fig. S4A–S4E). These observations support our reasoning that, beyond its robust

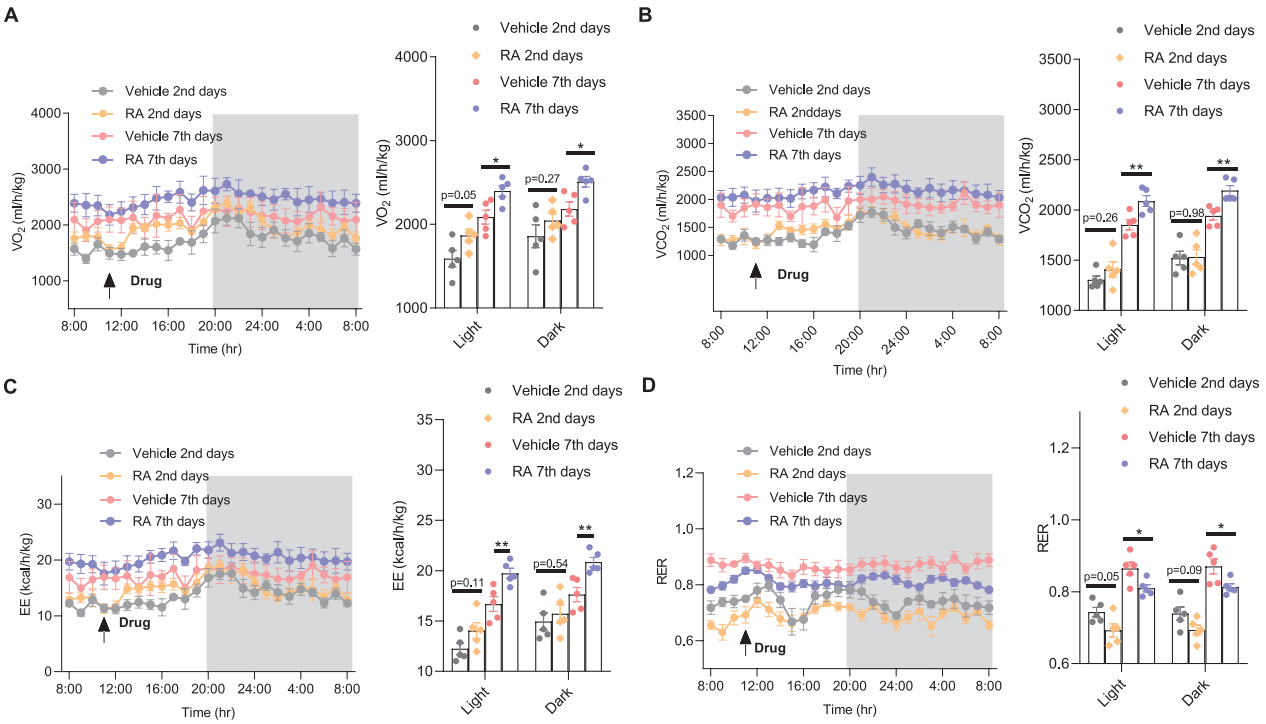

Figure 4. RA elevates EE.

DIO mice were placed in metabolic chambers after day 2 or 7 of RA (40 mg/kg, i.p.) or vehicle treatment. The arrow indicates the time of RA or vehicle intraperitoneal injection (n = 5 for each group). Indirect calorimetry was performed to quantify VO2 (A), VCO2 (B), EE (C), and RER (D). When DIO mice were treated with RA for 2 days, RA-treated DIO mice showed a trend of elevating EE. When DIO mice were treated with RA for 7 days, the EE of RA-treated DIO mice was significantly increased. Data are represented as mean ± SEM. P values were determined by Student's t-test (*P < 0.05, **P < 0.01, ***P < 0.001, ****P < 0.0001).

effects in reducing food intake, RA also functions in enhancing EE and shifts metabolism towards efficient utilization of fatty acids over glucose.

RA increased BAT thermogenesis and WAT browning in DIO mice

To further elucidate the mechanisms underlying RA, RNAseq, and transcriptomic analyses were performed in dissected hypothalamus from DIO mice with or without RA treatment. KEGG signaling pathway analysis showed that pathways relating to "regulation of lipolysis in adipocytes," "PI3K-Akt signaling pathway," "insulin signaling pathway" were enriched. Gene ontology analysis showed that terms relating to "ageing," "negative regulation of gluconeogenesis," "heat generation," and "negative regulation of lipid biosynthetic process" were enriched (Fig. S5A–S5C). These findings motivated further experiments to test the effect(s) of RA on BAT thermogenesis and glucose homeostasis.

Recalling our observations of increased EE in RA-treated DIO mice, it was notable that their overall physical movement (i.e., ambulatory activity) was actually reduced compared to vehicle control DIO model mice (Fig. S4F). This result supports that the observed increase in EE did not result from increased physical activity. As our GO analysis highlighted apparent activation of "heat generation," we examined whether RA-treated DIO mice had elevated BAT thermogenesis and/or WAT browning. Given that the thermoneutral conditions where mice no longer require thermogenesis to maintain body temperature can functionally downregulate the activity of BAT [37], we next explore the effect of RA for DIO housed at the thermoneutral environment. DIO mice treated with RA (thermoneutrality for mice) had a significantly less body weight reduction (Fig. 5A), but the percentage of the weight decreasing at 30°C was lower than the animals treated at room temperature (Fig. 5B). The food intake of RA-treated mice had slightly reduced (but significantly) compared with vehicle-treated DIO mice feeding at 30°C (Fig. 5C and 5D). Upon sacrificing the DIO mice feeding in 30°C, we observed that RA treatment had significantly reduced the weights of iWAT and pWAT, and there was no difference in eWAT, sWAT, and BAT (Fig. 5E). It is noted that the DIO mice treated with RA had a significantly less fat weight reduction at 30°C than the mice treated at room temperature. When maintained at room temperature (26°C), the core and skin temperature of the vehicle and RA-treated DIO mice are not different. However, the core and skin temperature of RA-treated mice were significantly higher than vehicle-treated mice after the mice were put in 4°C for 2 h after RA-treated for 3 days (Figs. 5F–5I and S5D–S5G).

Furthermore, we dissected adipose tissue in RA-treated DIO mice and control DIO mice and found increased clusters of

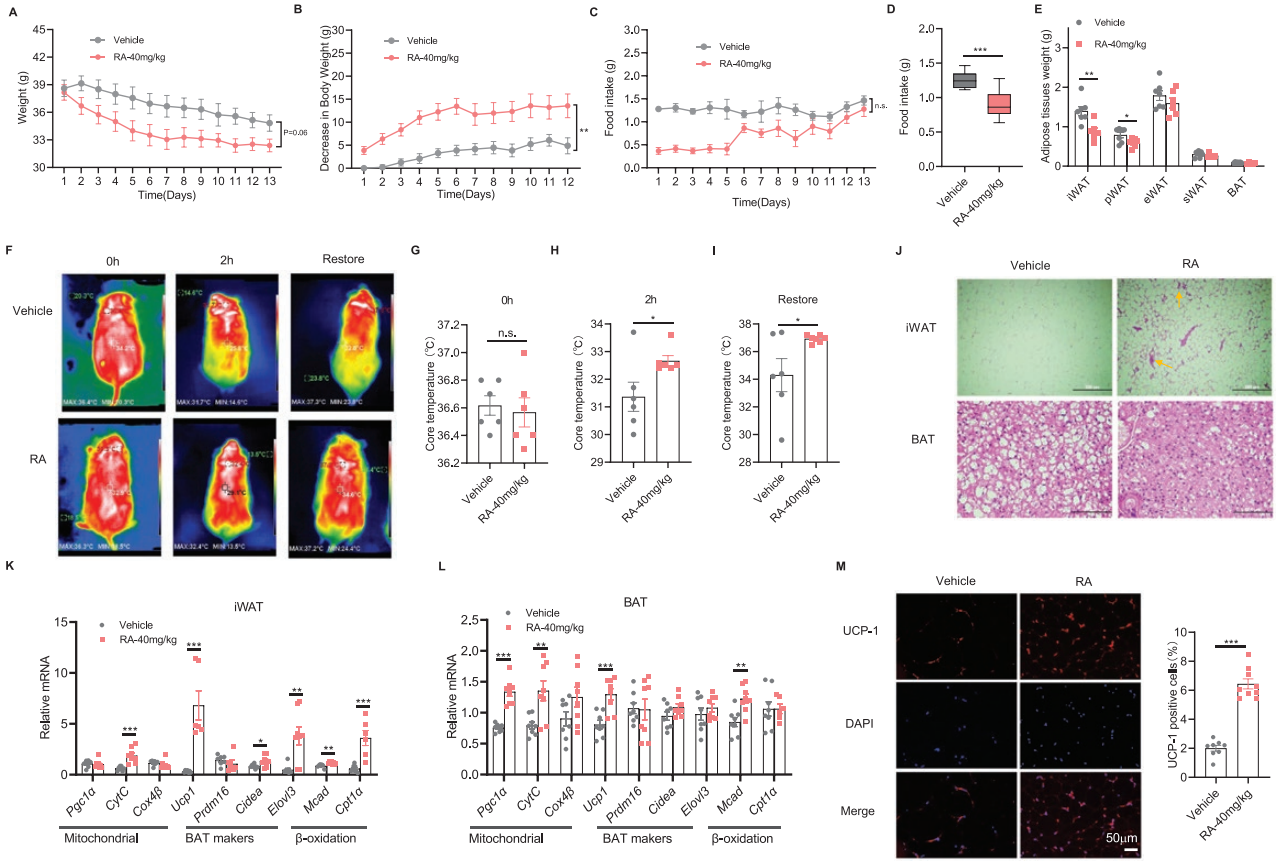

Figure 5. RA increases BAT thermogenesis and WAT browning in DIO mice.

(A–E) DIO mice were treated with vehicle or RA (40 mg/kg) intraperitoneally (i.p) for 2 weeks and housed at 30°C (n = 6). (A) Body weight, percent decrease (%) in body weight (B), food intake (C and D) and the weight of iWAT, pWAT, eWAT, sWAT, and BAT during treatment (E). (F–I) Core body temperature of the vehicle and RA-treated mice during cold challenge after hosed at room temperature (26°C) (n = 6). (J–M) DIO mice were treated with vehicle or RA (40 mg/kg) intraperitoneally (i.p) for 2 weeks at 22°C. (J) Representative HE staining of iWAT and BAT showed that adipose cell size was reduced in the RA-treated DIO mice. The scale bar indicates 200 μm. (K) qPCR analysis of the expression of thermogenic and brown fat genes in iWAT of DIO mice, showing that RA treatment promotes the expression of brown fat genes. (L) qPCR analysis of the expression of thermogenic and brown fat genes in BAT of DIO mice, showing that thermogenic genes were highly expressed after RA treatment (n = 8). (M) Immunofluorescence analysis of UCP-1 from iWAT sections of the vehicle or RA-treated DIO mice (left). Quantification of protein levels of UCP-1 in iWAT of the vehicle or RA-treated mice (right) (n = 3 per group). The scale bar indicates 50 μm. Data represented the mean ± SEM. P values were determined by Student's t-test (*P < 0.05, **P < 0.01, ***P < 0.001, ****P < 0.0001).

multilocular brown fat-like areas yet decreased unilocular white regions in the iWAT in the RA-treated animals (Fig. 5J). We also noted a trend that the size of the adipose cells was generally reduced in the RA-treated DIO mice (Fig. 5J). Furthermore, analysis of iWAT showed that the RA-treated DIO mice had an increased extent of browning (assessed as the amount of BAT in dissected iWAT (Fig. 5J). We also found that the number and size of fat droplets were significantly decreased in RA-treated DIO iWAT, indicating that RA treatment promoted utilization of iWAT-resident fat droplets. Next, we used qPCR to examine the expression of nine known browning-associated genes in iWAT and BAT of RA treated and vehicle control DIO model mice. The RA treatment significantly increased the expression of *CytC*, *UCP-1*, *Cidea*, *Elovl3*, *Mcad*, and *Cpt1α,* but has no changes of PKA related genes in iWAT (Figs. 5K and S5H–S5J), and significantly increased the expression of *Pgc1α*, *CytC*, *Cox4β*, *Ucp-1*, and *Mcad* in BAT (Fig. 5L). Further, immunofluorescence staining of iWAT confirmed that RA treatment promotes the accumulation of the Ucp-1 protein (aka Thermogenin), a mitochondrial carrier protein known to drive heat generation by uncoupling fatty acid oxidation from ATP production [38] (Fig. 5M). We further checked the expression of some factors that can induce *Ucp1* expression in iWAT. There was an uptrend in the expression of *Pparγ2* and *AP2* (but not significantly; Fig. S5K–S5O).

Considered together, these findings provide molecular-level evidence that RA stimulates both iWAT adipocyte browning and BAT thermogenesis explaining the weight reduction observed for the RA-treated DIO mice.

RA enhances glucose homeostasis of obese mice

We next investigated the effect of RA on glucose metabolism. A glucose tolerance test (GTT) revealed significantly faster disposal

of glucose from the circulation in the RA-treated mice with DIO, as compared to the vehicle-treated group (Fig. S6A and S6B). Insulin sensitivity, assayed using an insulin tolerance test, was also improved in the DIO mice after 2 weeks of RA treatment (Fig. S6C and S6D). We also found that the blood glucose level at 9 h fasting was significantly lower in the RA-treated DIO mice compared to the vehicle-treated group (Fig. S6E). Similar results were obtained for RA-treated db/db mice in comparison to their controls (Fig. S6F–S6J). Similarly, we checked the GTT of DIO mice treated with vehicle or RA feeding in 30°C, and found that RA slightly reduced the AUC of GTT (but not significantly; Fig. S6K–S6M). Furthermore, in the ob/ob mice, the RA + leptin group significantly reduced the blood glucose of ob/ob mice, indicating again RA is a leptin sensitizer (Fig. S6N–S6P). Since the insulin signaling pathway is involved in glucose metabolism. we further checked the IRS phosphorylation of the liver in DIO mice treated with vehicle or RA. The phosphorylation of IRS in the RA-treated group significantly increased, as compared with vehicle-treated group (Fig. S6Q and S6R). To sum up, these findings highlighted the attractive potential of RA as a candidate antidiabetic.

RA activates the hypothalamic leptin receptor-Stat3 pathway in DIO mice by inhibiting PTP1B and TCPTP

We next employed a similarity ensemble approach (SEA) [39] analysis to predict the potential target proteins of RA. Given that protein-tyrosine phosphatase 1B (PTP1B), a known negative regulator of the insulin signaling pathway, was among the top SEA prediction hits, we performed surface plasmon resonance analysis (SPR) with the human ortholog PTP1B to further characterize the apparent interaction of RA with this enzyme. Briefly, we detected K_d for RA and PTP1B was 51.3 μM (Fig. 6A and 6B). We also performed substrate titration studies using the known PTP1B substrate paranitrophenyl-phosphate (pNPP), and our finding that RA produced a reduction in the V_{max} but not in the K_m (Fig. 6C and 6D) clearly indicated that RA is a noncompetitive inhibitor of PTP1B. Supporting this, assays with truncation variants of human PTP1B—all of which still retain the known active site—were performed to identify the binding fragment. Our finding that RA is a more potent inhibitor of $PTP1B_{1\text{-}393}$ (Fig. 6E) compared to $PTP1B_{1\text{-}321}$ and $PTP1B_{1\text{-}298}$ supported that PTP1B's C-terminus participates in the observed noncompetitive inhibition of PTP1B by RA (Fig. 6F and 6G).

Then we performed molecular docking to predict the allosteric binding site of PTP1B (Fig. 6H) and TCPTP (Fig. S7G) targeted by RA and characterize the key interactions and residues involved in the binding model. The docking model reveals that RA binds to a site formed by helices α3 and α6. The nonpolar pentacyclic structure of RA binds in a hydrophobic pocket formed by the side chains of Leu192, Phe196, Phe280, and Ile281 (Fig. 6H). The carboxyl group of RA was close to Lys197 to form one hydrogen bond. The hydrophobic pocket formed by Leu192, Phe196, and Phe280 were also observed in other allosteric inhibitors targeted to PTP1B [40, 41].

Previous studies have revealed the JAK2 and STAT3 proteins function downstream of PTP1B, TCPTP, and leptin in regulating obesity and diabetes [16, 42, 43]. Specifically, the phosphorylated form of JAK2 recruits the transcription factor STAT3, which becomes phosphorylated by pJAK2, causing pSTAT3 homodimerization and its subsequent translocation into the nucleus [16, 44–46]. We therefore examined the expression and phosphorylation of these molecules after RA treatment and found that dissected hypothalamus tissues from RA-treated DIO mice had significantly increased levels of $JAK2^{Tyr1077}$ and $STAT3^{Tyr705}$ (Fig. 6I). Immunofluorescence analysis of hypothalamus sections using phosphorylation-sensitive antibodies also showed that the fluorescence intensity of $pSTAT3^{Tyr705}$ and the number of positive cells indeed increased significantly in RA-treated DIO mice (Fig. 6J and 6K). Considering that leptin acts on the arcuate nucleus of the hypothalamus to suppress food intake and promote EE [6], we further examined whether RA could cross the blood–brain barrier (BBB). HPLC assays showed that RA could across the BBB, peak at 0.5 h in the brain tissue and gradually disappear after 2 h (Fig. S7H). It also accumulated in the liver and iWAT, which peaked at 0.5 h in the liver (Fig. S7I) and peaked at 1 h in the iWAT (Fig. S7J). Given that poor cell permeability of PTP1B inhibitors limits their ability to reach the intracellular target [47], HPLC assay was therefore used to measure the ratio of RA in Caco-2 cell. We found that RA was a highly permeable drug, as the atenolol and propranolol were used as low- and high-permeability controls (Fig. S7K and S7L).

Considered together, these results provided a possibility that RA could across the BBB to inhibit the PTP1B and TCPTP in brain cell to increase leptin and insulin sensitivity, repress the feeding, increase browning, decrease adiposity, and improve glucose metabolism.

PTP1B knockdown leads to lifespan extension

Considering that RA is a leptin sensitizer, so we hypothesized that RA may play an anti-aging role as a leptin sensitizer. Next, we tested other leptin sensitizers [such as celastrol and withaferin A (WA)] for their role in anti-aging. Subsequent assessment of lifespan in the presence of celastrol or WA showed that two leptin sensitizers significantly extended the lifespan of yeast to a similar extent (Fig. 7A and 7B). A previous study has revealed that celastrol showed markedly more effectiveness against PTP1B than TCPTP [48], we also found WA can inhibit PTP1B activity (Fig. S7M and S7P), but the anti-aging effect of RA on yeast (Fig. 1B, 19.35 generations) is better than either celastrol (Fig. 7A, 12.01 generations) or WA (Fig. 7B, 14.79 generations). Our observations about leptin sensitizers with PTP1B inhibition activity supported our reasoning that RA may play an anti-aging role by inhibiting PTP1B. First of all, we used yeast to check for the relationship between the anti-aging effect of RA and yPTP1 (PTP1B allelic gene in yeast). We found deletion of yPTP1 in yeast totally abolished any lifespan extension phenotype from RA treatment

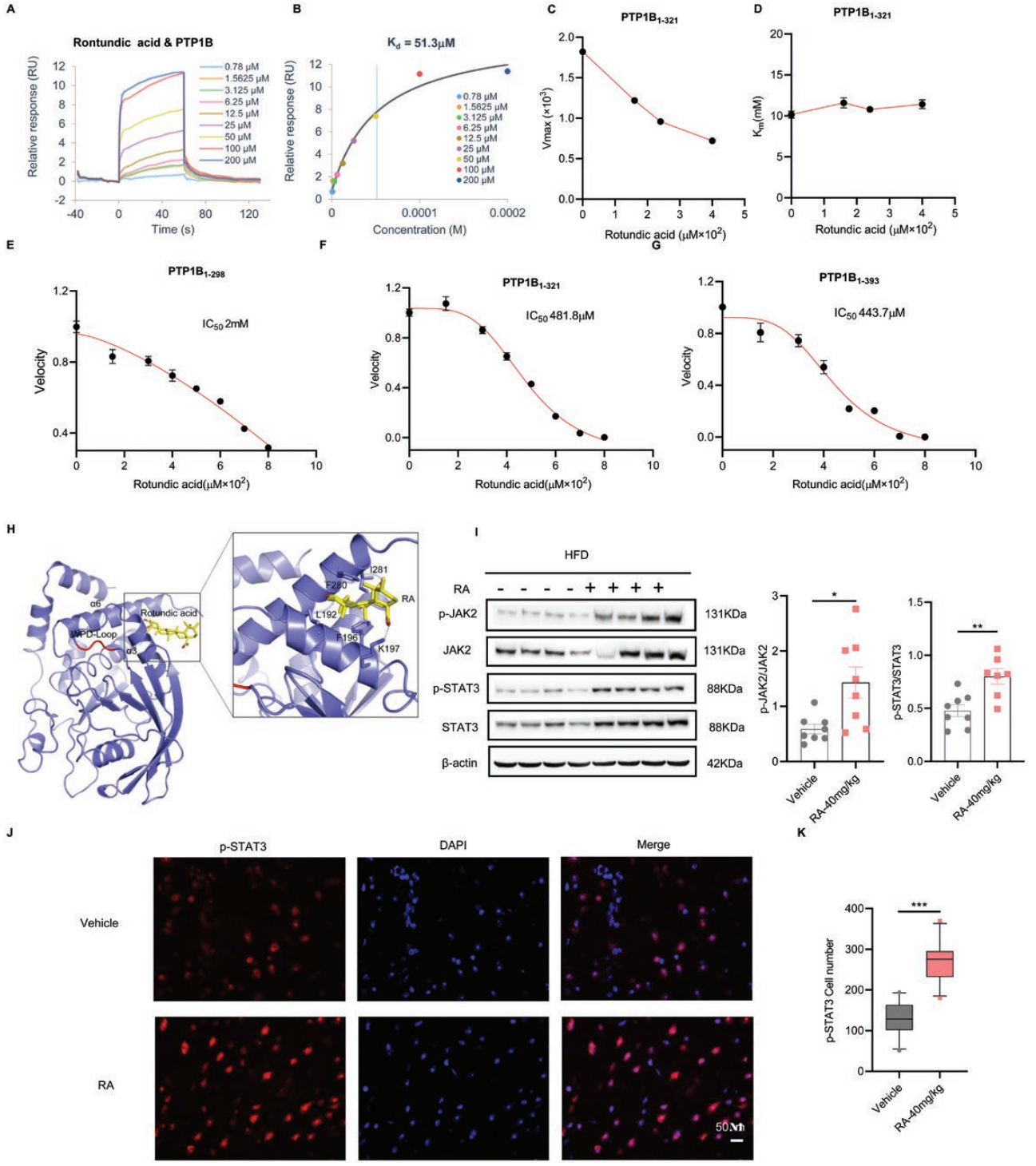

Figure 6. RA targets PTP1B and TCPTP and potentiates leptin signaling.

(A and B) Surface plasmon resonance analysis of the interaction between RA and PTP1B. RA in PBSP-5% DMSO buffer was injected over a CM5 sensor chip surface to which human PTP1B was immobilized. The response units (RU) were corrected to a reference flow cell. (C–G) Substrate titration reveals that RA is a noncompetitive inhibitor of PTP1B that inhibits substrate catalysis (V_{max}) but not substrate binding (constant K_m). (C) Plots of V_{max}. (D) Plot of K_m (n = 3 per group). (E–G) *In vitro* enzyme kinetic studies with his-tagged purified human PTP1B showed RA inhibition (n = 3 per group). Inhibition curves of $PTP1B_{1-298}$ (E), $PTP1B_{1-321}$ (F), and $PTP1B_{1-393}$ (G) variant (with the active site) in the presence of RA with pNPP. (H) The top-ranked binding model of autodocking for PTP1B (PDB:6B8Z) and RA. RA is shown in a yellow stick model; the hydrogen bond is shown by a black dashed line. (I–K) Vehicle (n = 8) or RA (40 mg/kg) (n = 8) were administered to DIO mice. (I) RA induced $JAK2^{Tyr1007}$ and $STAT3^{Tyr705}$ phosphorylation detected by immunoblot analysis (left). The total protein was extracted from dissected hypothalamus tissues from DIO mice. The ratio of signal intensities of p-$JAK2^{Tyr1007}$ to total JAK2 (middle) and the ratio of signal intensities of

(Fig. 7C), indicating yPTP1 is essential in the observed lifespan extension effects of RA. Moreover, deletion of yPTP1 in yeast in the presence of celastrol or WA totally abolished the lifespan extension effects (Fig. 7D and 7E). These results emphasize that inhibition of PTP1B could delay aging processes.

As PTP1B is important for the regulation of proliferation, immune, and metabolism [49, 50], we hypothesized that while the deletion of this gene does not improve lifespan [51], a partial knockdown of it may do so. We therefore mated the WT and PTP1△strains to generate a heterozygous diploid yeast strain with a single copy of PTP1. We found that this partial PTP1 knockdown significantly extended lifespan relative to the control BY4743 strain (Fig. 7F). In human cell lines, we found that KY226 (PTP1B inhibitor) mediated PTP1B activity inhibition was able to rejuvenate senescent cells, and there were no obvious superposition lifespan extension effects in the KY226 combined with RA group (Fig. 7G and 7H), thus strongly suggesting overlap in their targeting and activity.

Next, we used siRNA to achieve PTP1B knockdown in human cell lines and found that siRNA-mediated PTP1B knockdown was able to rejuvenate senescent cells with SA-β-gal staining being used to quantify senescence (Fig. 7I and 7J). We further used qPCR to examine the expression of senescence-associated secretory phenotype (SASP)-related genes, PTP1B knockdown significantly reduced the expression of *IL-6*, *MMP3*, *P21,* and *WNT16B* (Fig. 7K). In addition, Western blot analysis further confirmed the downregulation of P21 that is highly expressed in senescent cells at the protein level in the PTP1B knockdown strain (Fig. 7L). In summary, RA function apparently depends on PTP1B in human cell lines, and the inhibition of PTP1B proteins can mitigate aging-related effects in these cells.

Discussion

In this study, we found RA confers both anti-aging and anti-obesity effects (Fig. 8). RA treatment extended the lifespan of yeast by 135%, and long-term experiments in mice increased by 16.2% total and 44.2% in residual lifespan. Accounting for the observed weight decreases, we found that RA reduced food intake while also boosting fat consumption of DIO mice, and observed that RA increased EE, BAT thermogenesis, WAT browning, and enhanced glucose metabolism in DIO mice, which indirectly proved that muscle associated with fat and sugar metabolism, since RA screened based on aging-related genes identified by muscle tissues showed the effect of regulating fat metabolism. Simultaneously, we showed several lines of evidence supporting that RA improves leptin sensitivity, specifically by acting as a noncompetitive inhibitor targeting the C-terminus of the PTP1B enzyme. Moreover, considering the anti-aging effect of RA, we also found PTP1B knockdown can reduce senescence.

Previous studies have shown that deletion of PTP1B and TCPTP in the hypothalamic of obese mice enhances hypothalamic leptin and insulin signaling and contributes to the maintenance of obesity, driving brown and/or beige adipocyte thermogenesis, and EE [52, 53]. In our study, inhibition of PTP1B and TCPTP by RA achieved the same trend of weight loss (26% in 40 g and 55 g mice). We showed four pieces of evidence PTP1B and TCPTP are the mode of action targets of RA. (i) RA directly binds to PTP1B verified by SPR. (ii) RA modulates the enzymatic activity of PTP1B and TCPTP variants. (iii) RA activated the hypothalamic JAK2-STAT3 pathway in DIO mice. (iv) The phosphorylation of IRS, a target of PTP1B was increased by RA in liver of DIO mice. We identified that the inactivation of PTP1B and TCPTP led by RA promoted leptin and insulin signaling and eventually promotes WAT browning and EE. We also observed that RA treatment decreased RER indicated elevated fat consumption, and improved glucose metabolism. All of these results provide the possibility in support of a role for RA in reducing obesity by inhibiting PTP1B and TCPTP activity which increases leptin sensitivity. It has been reported that serine phosphorylation of PTP1B was significantly increased with aging [54], and PTP1B was downregulated by SIRT1. Notably, the dependence of RA upon PTP1(B) also suggests that PTP1B may be a potent target for aging. We showed three pieces of evidence inhibiting PTP1(B) could extend lifespan. (i) yPTP1 deletion in yeast totally abolished the lifespan extension of RA, celastrol or WA, noting that these compounds all have PTP1B inhibition activity. (ii) partial PTP1 knockdown significantly extended lifespan relative to the control BY4743 strain. (iii) KY226 mediated PTP1B activity inhibition or PTP1B knockdown using siRNA was able to rejuvenate the senescent cell.

Research limitations

However, our study has some research limitations. First, RA's effect should be checked in PTP1B, TCPTP, and PTP1B/TCPTP deleted mice. RA could significantly reduce the ALT and AST of DIO mice at room temperature and 30°C, indicating the powerful anti-inflammation effects. Therefore, we believe that RA has other potential targets, such as some target proteins related to inflammation. Second, more investigations are needed to reveal how to increase the Ucp-1 through inhibition of TCPTP and PTP1B and the role of Ucp1 in aging. Furthermore, there are some resolved questions about the RA, such as its insolubility as well as lower bioavailability. Besides, although we have identified RA as a highly permeable drug and could across the BBB, the dose of RA in our study is a little high. Though 40 mg/kg RA has not significant side-effect on liver for 14 days, it may lead to damage to liver if mice receive 40 mg/kg RA treatment

p-STAT3^{Tyr705} to total STAT3 (right). (J and K) Immunofluorescence analysis of p-STAT3^{Tyr705} from marine hypothalamus sections using phosphorylation-sensitive antibodies (J) and quantification of p-STAT3^{Tyr705} positive cells (K). The scale bar indicates 50 μm, $n = 3$ per group. Data are represented as the mean ± SEM. P values were determined by Student's t-test (*$P < 0.05$, **$P < 0.01$, ***$P < 0.001$).

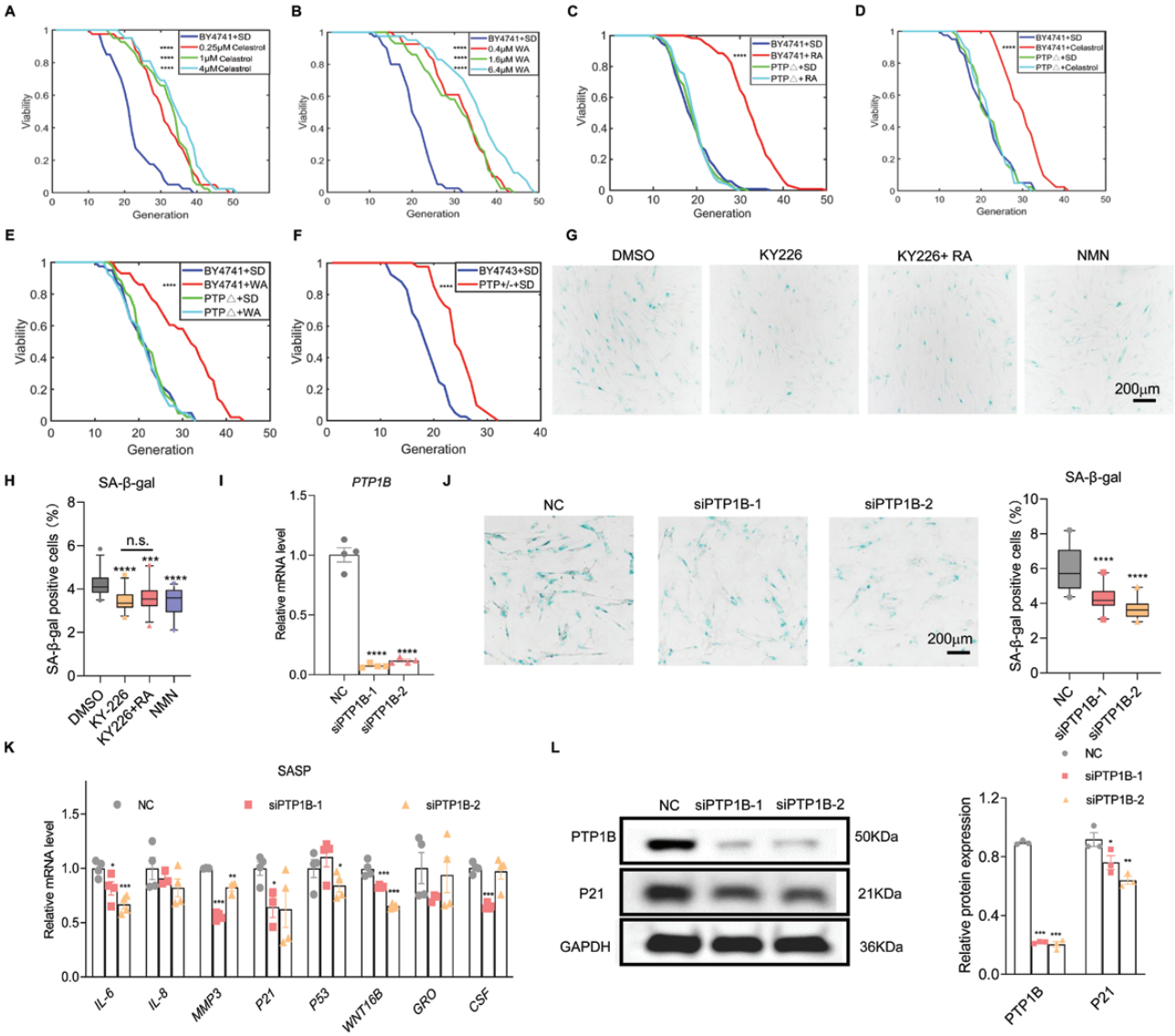

Figure 7. PTP1B knockdown leads to lifespan extension.

(A and B) Celastrol (A) or WA (B) affects the lifespan of WT cell strains (The lifespan of 40 yeast cells were counted for each group). (C–E) RA (C), celastrol (D), and WA (E) effects on WT or PTP1△deletion cell strains (The lifespan of 40 yeast cells were counted for each group). RA-treated wild-type mother cells showed a prolonged replicative lifespan compared to untreated cells (growth on SD medium); in contrast, no prolonged replicative lifespan phenotype was observed when PTP1△yeast cells were treated with RA. (F) Heterozygous diploid cell lifespan for PTP1$^{+/-}$ and BY4743 strains (The lifespan of 40 yeast cells were counted for each group). (G and H) Quantification of WI-38 cells stained for SA-β-gal staining following 5 μM KY226, 5 μM KY226 and 10 μM RA, 1 mM NMN or DMSO vehicle treatment (the scale bar indicates 200 μm, $n = 3$ per group). (I) The expression of PTP1B in control or PTP1B knockdown WI-38 cells ($n = 4$). (J) Quantification of SA-β-gal staining in PTP1B knockdown WI-38 cells ($n = 4$). (K) qPCR analysis of the expression of SASP-related gene ($n = 4$). (L) The expression of PTP1B and p21 was detected by immunoblot analysis ($n = 3$). Data are represented as the mean ± SEM. *P* values were determined by one-way ANOVA test (*$P < 0.05$, **$P < 0.01$, ***$P < 0.001$).

for >2 weeks, thereby it is necessary to explore the safety of RA with long-term treated. Simultaneously, the deeper understanding of the relationship between PTP1B and aging should be done, as we only emphasized the effects of PTP1B knockdown in cell level. It seems likely that developing and testing derivatives using RA as a lead compound will yield increased inhibitory performance and deepen our understanding of the biology of aging and obesity.

Materials and methods

RA

RA was purchased from DESITE Biotechnology Co., Ltd (NO. 20157-57-5), Chengdu, China. The average molecular weight was ~488.71 Da, as determined by high-performance steric exclusion chromatography analysis. RA was dissolved in 2% DMSO and 0.5% CMC-Na for the *in vivo* experiments in our experiments.

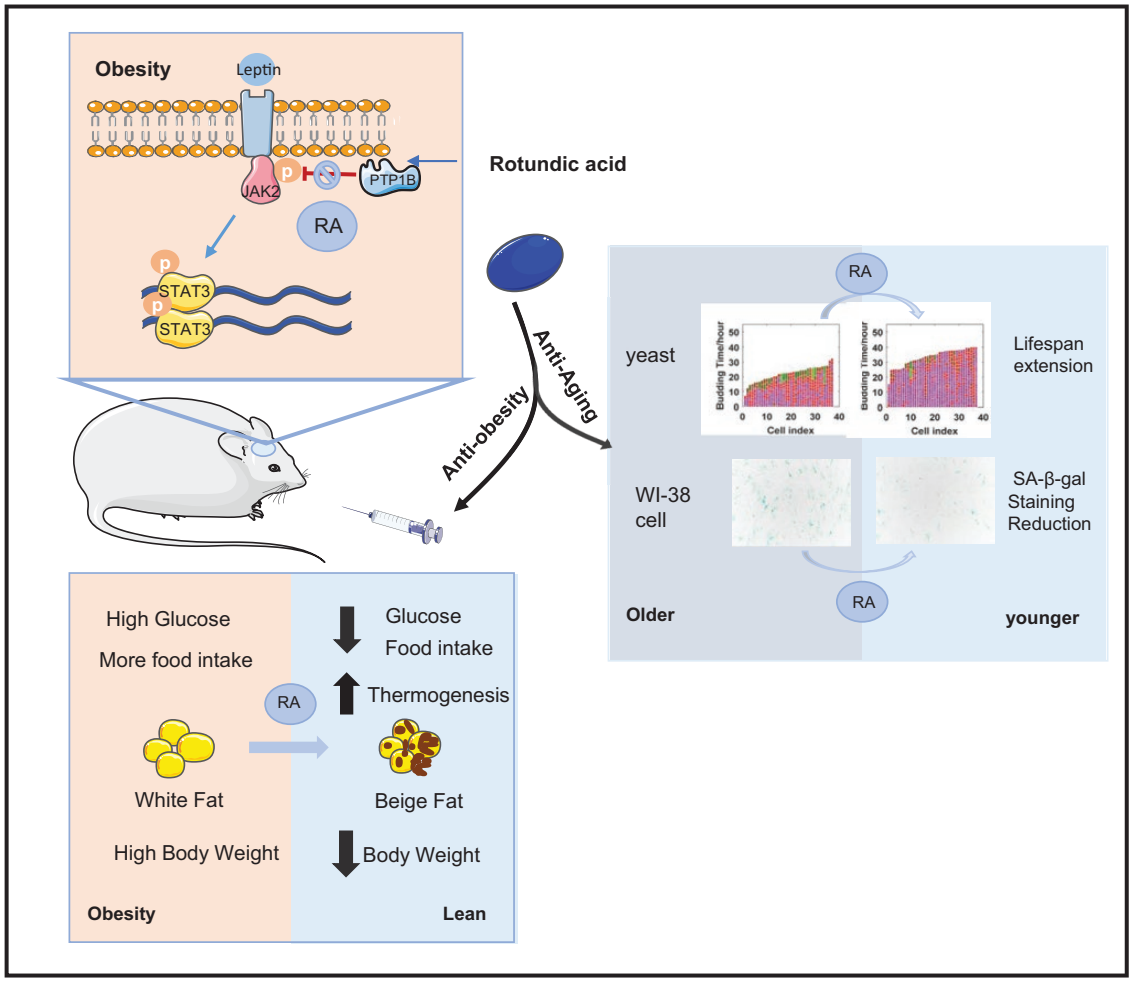

Figure 8. The summary of this study.

Animal studies

Animal experiments were performed in strict accordance with the Ethics Committee of Peking University Health Science Center (PKUHSC; LA2016113) and approved by the Animal Care and Use Committee of Peking University. C57BL/6N, db/db mice were obtained from the Department of Laboratory Animal Science of Peking University Health Science Center and the Charles River Laboratories Beijing Branch. For a generation of DIO mice, wild-type lean C57BL/6N male mice were placed on a 60 kcal% High Fat Diet (Research Diets, D12492i) at the age of 8 weeks. All other animals were maintained on a chow diet (13.5% from fat calories; Lab Diet). Animals were housed under 12 h of light and 12 h of the dark cycle with unrestricted access to food and water unless otherwise described. Naturally aged mice were purchased from SPF Biotechnology Co., Ltd, Beijing, China. For C57BL/6N mice, starting from 16 months, a week of intraperitoneal injection treatment is given every month, the dosage is 40 mg/kg, administration time for 6 months, the control group was assigned 0.5% sodium carboxymethyl cellulose, and the death of the mice was recorded.

Administration of RA

RA was dissolved in 0.5% CMC-Na. For intraperitoneal (i.p.) treatment, mice received 10/20/40 mg/kg RA for 2-weeks. Vehicle groups received 0.5% CMC-Na according to mice's weight.

PTP1B gene silencing

To silence PTP1B, cells were transfected with appropriate siRNA using Lipofectamine 3000 (ThermoFisher Scientific). GenePharma (Shanghai) has prepared human siRNA against PTP1B with the following sequence:

PTP1B siRNA1: sense: GAUGGAGAAAGGUUCGUUATT;
antisense: UAACGAACCUUUCUCCAUCTT.
PTP1B siRNA2: sense: GACCCUUCUUCCGUUGAUATT;
antisense: UAUCAACGGAAGAAGGGUCTT.

Statistical analysis

Data are presented as mean ± SEM. Statistical significance was calculated by Student's *t*-test or by one-way ANOVA. Significance was accepted at $^{*}P < 0.05$, $^{**}P < 0.01$, $^{***}P < 0.001$, $^{****}P < 0.0001$.

Data availability

Data available within the article or its supplementary materials.

Supplementary data

Supplementary material is available at *Life Medicine* online.

Acknowledgements

This work was supported by the National Key R&D Program of China (Grant No. 2018YFA0900200), National Natural Science Foundation of China (NSFC) (Grant Nos. 32170756, 81903539), and Beijing Municipal Natural Science Foundation (Grant No. 5182012).

Author contributions

J.Z. and X.W. (experiments and analysis of obesity), J.Z. and Y.P.A (experiments and analysis of aging). J.Z., S.J.Z., and W.K. conducted enzyme kinetic studies and docking. J.Z and L.T.H purified the PTP1B and TCPTP protein. M.M.G performed DLEPS screening for the anti-aging drug. J.Z. and Z.W.X. wrote the manuscript. Z.W.X. and S.J.Z. supervised the team.

Conflict of interest

The authors declare no competing interests.

References

1. Kranjac AW, Wagmiller RL. Association between age and obesity over time. *Pediatrics* 2016;137:e20152096
2. Pi-Sunyer X. The medical risks of obesity. *Postgrad Med* 2009;121:21–33
3. Wang YC, McPherson K, Marsh T, et al. Health and economic burden of the projected obesity trends in the USA and the UK. *Lancet* 2011;378:815–25
4. Reuser M, Bonneux L, Willekens F. The burden of mortality of obesity at middle and old age is small. A life table analysis of the US Health and Retirement Survey. *Eur J Epidemiol* 2008;23:601–7
5. Fontaine KR, Redden DT, Wang C, et al. Years of life lost due to obesity. *JAMA* 2003;289:187–93
6. Dietrich MO, Horvath TL. Hypothalamic control of energy balance: insights into the role of synaptic plasticity. *Trends Neurosci* 2013;36:65–73
7. Myers MG, Cowley MA, Munzberg H. Mechanisms of leptin action and leptin resistance. *Annu Rev Physiol* 2008;70:537–56
8. Lee J, Liu J, Feng X, et al. Withaferin A is a leptin sensitizer with strong antidiabetic properties in mice. *Nat Med* 2016;22:1023–32
9. Liu J, Lee J, Salazar Hernandez MA, et al. Treatment of obesity with celastrol. *Cell* 2015;161:999–1011
10. Considine RV, Sinha MK, Heiman ML, et al. Serum immunoreactive-leptin concentrations in normal-weight and obese humans. *N Engl J Med* 1996;334:292–5
11. Finucane MM, Stevens GA, Cowan MJ, et al. National, regional, and global trends in body-mass index since 1980: systematic analysis of health examination surveys and epidemiological studies with 960 country-years and 9.1 million participants. *Lancet* 2011;377:557–67
12. Scarpace PJ, Tumer N. Peripheral and hypothalamic leptin resistance with age-related obesity. *Physiol Behav* 2001;74:721–7
13. Scarpace PJ, Matheny M, Moore RL, et al. Impaired leptin responsiveness in aged rats. *Diabetes* 2000;49:431–5
14. Carter S, Caron A, Richard D, et al. Role of leptin resistance in the development of obesity in older patients. *Clin Interv Aging* 2013;8:829–44
15. Chellappa K, Perron IJ, Naidoo N, et al. The leptin sensitizer celastrol reduces age-associated obesity and modulates behavioral rhythms. *Aging Cell* 2019;18:e12874
16. St-Pierre J, Tremblay ML. Modulation of leptin resistance by protein tyrosine phosphatases. *Cell Metab* 2012;15:292–7
17. Elchebly M, Payette P, Michaliszyn E, et al. Increased insulin sensitivity and obesity resistance in mice lacking the protein tyrosine phosphatase-1B gene. *Science* 1999;283:1544–8
18. Klaman LD, Boss O, Peroni OD, et al. Increased energy expenditure, decreased adiposity, and tissue-specific insulin sensitivity in protein-tyrosine phosphatase 1B-deficient mice. *Mol Cell Biol* 2000;20:5479–89
19. Lopez-Otin C, Blasco MA, Partridge L, et al. The hallmarks of aging. *Cell* 2013;153:1194–217
20. Gagarina V, Gabay O, Dvir-Ginzberg M, et al. SirT1 enhances survival of human osteoarthritic chondrocytes by repressing protein tyrosine phosphatase 1B and activating the insulin-like growth factor receptor pathway. *Arthritis Rheum* 2010;62:1383–92
21. Sun C, Zhang F, Ge X, et al. SIRT1 improves insulin sensitivity under insulin-resistant conditions by repressing PTP1B. *Cell Metab* 2007;6:307–19
22. Tiganis T. PTP1B and TCPTP--nonredundant phosphatases in insulin signaling and glucose homeostasis. *FEBS J* 2013;280:445–58
23. Loh K, Fukushima A, Zhang X, et al. Elevated hypothalamic TCPTP in obesity contributes to cellular leptin resistance. *Cell Metab* 2011;14:684–99
24. Zhang Z, Zhang H, Li B, et al. Berberine activates thermogenesis in white and brown adipose tissue. *Nat Commun* 2014;5:5493
25. Dang Y, An Y, He J, et al. Berberine ameliorates cellular senescence and extends the lifespan of mice via regulating p16 and cyclin protein expression. *Aging Cell* 2020;19:e13060
26. Xia B, Shi XC, Xie BC, et al. Urolithin A exerts antiobesity effects through enhancing adipose tissue thermogenesis in mice. *PLoS Biol* 2020;18:e3000688
27. Ryu D, Mouchiroud L, Andreux PA, et al. Urolithin A induces mitophagy and prolongs lifespan in C. elegans and increases muscle function in rodents. *Nat Med* 2016;22:879–88
28. Thang TD, Kuo PC, Yu CS, et al. Chemical constituents of the leaves of Glochidion obliquum and their bioactivity. *Arch Pharm Res* 2011;34:383–9
29. He YF, Nan M-L, Sun J-M, et al. Synthesis, characterization and cytotoxicity of new rotundic acid derivatives. *Molecules* 2012;17:1278–91
30. Zhu J et al. Prediction of drug efficacy from transcriptional profiles with deep learning. *Nat Biotechnol* 2021;39:1444–52
31. Zahn JM et al. Transcriptional profiling of aging in human muscle reveals a common aging signature. *PLoS Genet* 2006;2:e115
32. Xie Z et al. Molecular phenotyping of aging in single yeast cells using a novel microfluidic device. *Aging Cell* 2012;11:599–606
33. *WHO methods and data sources for country-level causes of death 2000–2019 (Global Health Estimates Technical Paper WHO/DDI/DNA/GHE/2020.2)*
34. Dalamaga M et al. Leptin at the intersection of neuroendocrinology and metabolism: current evidence and therapeutic perspectives. *Cell Metab* 2013;18:29–42
35. Halaas JL et al. Physiological response to long-term peripheral and central leptin infusion in lean and obese mice. *Proc Natl Acad Sci USA* 1997;94:8878–83
36. Friedman JM, Halaas JL. Leptin and the regulation of body weight in mammals. *Nature* 1998;395:763–70
37. Bal NC et al. Sarcolipin is a newly identified regulator of muscle-based thermogenesis in mammals. *Nat Med* 2012;18:1575–9

38. Cypess AM et al. Identification and importance of brown adipose tissue in adult humans. *N Engl J Med* 2009;360:1509–17
39. Keiser MJ et al. Relating protein pharmacology by ligand chemistry. *Nat Biotechnol* 2007;25:197–206
40. Wiesmann C et al. Allosteric inhibition of protein tyrosine phosphatase 1B. *Nat Struct Mol Biol* 2004;11:730–7
41. Keedy DA et al. An expanded allosteric network in PTP1B by multitemperature crystallography, fragment screening, and covalent tethering. *Elife* 2018;7:e36307
42. Zabolotny JM et al. PTP1B regulates leptin signal transduction in vivo. *Dev Cell* 2002;2:489–95
43. Bence KK et al. Neuronal PTP1B regulates body weight, adiposity and leptin action. *Nat Med* 2006;12:917–24
44. Garofalo C, Surmacz E. Leptin and cancer. *J Cell Physiol* 2006;207:12–22
45. Ghilardi N, Skoda RC. The leptin receptor activates janus kinase 2 and signals for proliferation in a factor-dependent cell line. *Mol Endocrinol* 1997;11:393–9
46. Vaisse C et al. Leptin activation of Stat3 in the hypothalamus of wild-type and ob/ob mice but not db/db mice. *Nat Genet* 1996;14:95–7
47. Maheshwari N, Karthikeyan C, Trivedi P, et al. Recent advances in protein tyrosine phosphatase 1B targeted drug discovery for type II diabetes and obesity. *Curr Drug Targets* 2018;19:551–75
48. Kyriakou E et al. Celastrol promotes weight loss in diet-induced obesity by inhibiting the protein tyrosine phosphatases PTP1B and TCPTP in the Hypothalamus. *J Med Chem* 2018;61:11144–57
49. Yip SC, Saha S, Chernoff J. PTP1B: a double agent in metabolism and oncogenesis. *Trends Biochem Sci* 2010;35:442–9
50. Xu H et al. Phosphatase PTP1B negatively regulates MyD88- and TRIF-dependent proinflammatory cytokine and type I interferon production in TLR-triggered macrophages. *Mol Immunol* 2008;45:3545–52
51. Le Sommer S et al. Deficiency in protein tyrosine phosphatase PTP1B shortens lifespan and leads to development of acute leukemia. *Cancer Res* 2018;78:75–87
52. Dodd GT et al. Intranasal targeting of hypothalamic PTP1B and TCPTP reinstates leptin and insulin sensitivity and promotes weight loss in obesity. *Cell Rep* 2019;28:2905–2922. e2905
53. Dodd GT et al. Leptin and insulin act on POMC neurons to promote the browning of white fat. *Cell* 2015;160:88–104
54. Garcia-San Frutos M et al. Involvement of protein tyrosine phosphatases and inflammation in hypothalamic insulin resistance associated with ageing: effect of caloric restriction. *Mech Ageing Dev* 2012;133:489–97